An LFT Approach to H_∞ Control Design for Diesel Engine Common Rail Injection System

Christophe Gauthier, Olivier Sename, Luc Dugard, G. Meissonnier

Oil & Gas Science and Technology – Rev. IFP, Vol. 62 (2007), No. 4, pp. 513-522

DOI: 10.2516/ogst:2007046

IFP International Conference
Rencontres Scientifiques de l'IFP

New Trends on Engine Control, Simulation and Modelling
Avancées dans le contrôle et la simulation des systèmes Groupe Moto-Propulseur

An LFT Approach to H_∞ Control Design for Diesel Engine Common Rail Injection System

C. Gauthier[1,2], O. Sename[1], L. Dugard[1] and G. Meissonnier[2]

1 GIPSA-lab (Control Systems Dept., former LAG), INPG-CNRS UMR 5216, ENSIEG, BP 46, 38402 Saint Martin d'Hères Cedex, France
2 Delphi Diesel Systems, 9 boulevard de l'industrie, 41042 Blois Cedex, France
e-mail: christophe.l.gauthier@delphi.com - olivier.sename@inpg.fr - luc.dugard@inpg.fr - guillaume.meissonnier@delphi.com

Résumé — Une approche LFT pour la commande H_∞ des systèmes d'injection "Common rail'' des moteurs Diesel — Dans cet article, une approche LFT est proposée pour concevoir un contrôleur H_∞ LPV à temps-discret incluant une compensation anti-saturation. Cette méthodologie est appliquée au système d'injection "Common Rail" des moteurs Diesel à injection directe. L'efficacité de ce contrôleur est mise en avant en le comparant à l'aide de simulations avec un régulateur de type PID à gain séquencé embarqué sur véhicule.

Abstract* — *An LFT Approach to H_∞ Control Design for Diesel Engine Common Rail Injection System — *In this paper, a linear fractional transformation (LFT) approach is proposed in order to design a linear parameter-varying discrete-time H_∞ controller including an anti-windup compensation. The provided methodology is applied to the control of diesel engine common rail injection systems. Simulation results on a non linear model are then shown and discussed. The control method is briefly compared with the on-board gain-scheduled PID controller.*

INTRODUCTION

In the heart of sustainable development, engine control is a major field of automotive control systems and concerns many subsystems (idle, turbo, injection...). However the increasing complexity of such systems, necessary to meet the emissions and consumption requirements, has led to the need for advanced control methodologies (Gissinger and Le Fort-Piat, 2002; Kiencke and Nielsen, 2000; van Nieuwstadt, 2002). In particular, common rail systems have been developed to reduce noise, exhaust emissions and fuel consumption and, at the same time to increase performances. Furthermore such functionalities must be achieved, taking into account the system variations according to engine speed, fuel temperature, etc., and for all cars equipped with the common rail injection system.

The development of the embedded control scheme should then account for such non linearities and robustness requirements while remaining simple enough to be reusable for a wide range of products, by any control engineer and in a reasonable design time. One chose then to avoid specific design methods such as control gain calibration for each operating point which needs system identification and control design in a very wide range of running points. This paper concerns the development of an advanced control strategy for Common Rail injection system with the objective to reach better performance and robustness (due to pollution norm which are more and more restrictive, etc.), incorporating the non linear effects as varying parameters (Jung and Glover, 2006;

Zhang *et al.*, 2005). The so called LFT approach is used for control design in the H_∞ framework. On the other hand, one wishes to develop a *generic* model-based approach for the control design over the whole set of operating points.

The outline of the paper is as follows. Section 1 briefly describes the system and its corresponding models, in particular in the LFT form. Section 2 is devoted to the generic synthesis of a discrete-time H_∞ LFT controller. In Section 3, an anti-windup scheme is presented that successfully tackles the input saturation problem. Some simulation results are shown in Section 4.

1 COMMON RAIL SYSTEM

1.1 Presentation

The Common Rail system is an electronic injection system that offers a wide range of injection pressures independently of engine speed. The electronically driven injectors allow a flexible control of injection timing and delivery. It is able to split injection in up to 4 phases: 2 pre-injections (called *pilot injections*), a main injection and a post-injection. This system achieves a good level of performance, with a significant fuel economy and low exhaust emissions (Guerrassi and Dupraz, 1998).

The working principle of the common rail system is to inject a precise quantity of fuel at high pressure (Guerrassi *et al.*, 2002; Guerrassi and Dupraz, 1998). The pressure demand is mapped against several parameters, mainly engine speed and torque demand. Typical requirements on the pressure are variations from 230 bar up to 1600 bar within a tolerance of 1% and steep gradients (*e.g.* up to ± 3000 bar/s).

Five main components compose this system as shown in Figure 1. The first one is the rail which is a pressurized tank feeding the injectors. Then a high pressure (HP) pump, driven by the engine, fills the rail and increases its pressure. The higher the engine speed is, the greater the pump flow is. In order to control the pump flow, an inlet metering valve (IMV) is placed at the HP pump inlet. The fuel is injected through the injectors from the rail into cylinders, which means that this flow cannot be used for rail pressure control. The last component, the high pressure valve (HPV), allows to control the output flow of the rail.

1.2 Nonlinear modelling features

The following scheme *(Fig. 2)* emphasizes the interaction of the five components described previously. Q_{pmp} and Q_{hpv} depend on the inputs V_{imv} and V_{hpv}. The injector flow Q_{inj} is considered as a disturbance for the rail pressure control.

In the sequel, the considered control mode involves a single actuator: the IMV. Some other control modes may include both actuators (IMV and HPV) but they are not considered in this paper. This means that, for this study, $Q_{hpv} = 0$.

A complete non linear model of the system was proposed in (Gauthier *et al.*, 2005) as the interconnection of the models of the five subsystems. This model was validated on real data and may be used for control validation.

In this section only the part of this model dedicated to the rail behavior is briefly recalled in order to show the need for a Linear Parameter Varying model of the plant. The remaining subsystems, such as the IMV actuator or the HP pump, are modelled using physical equations (electrical, hydraulic and mechanical) and then linearized in a generic way to lead to LPV models.

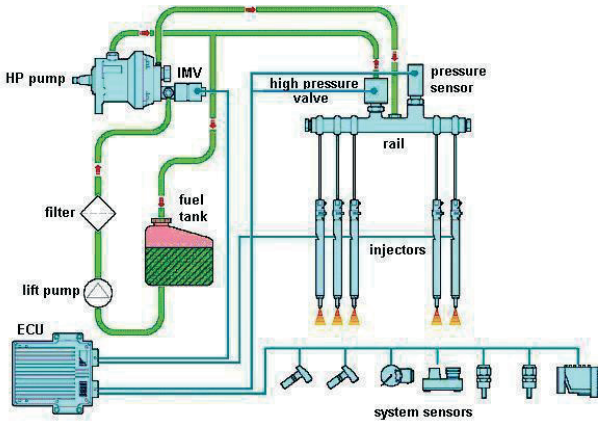

Figure 1

Common rail system.

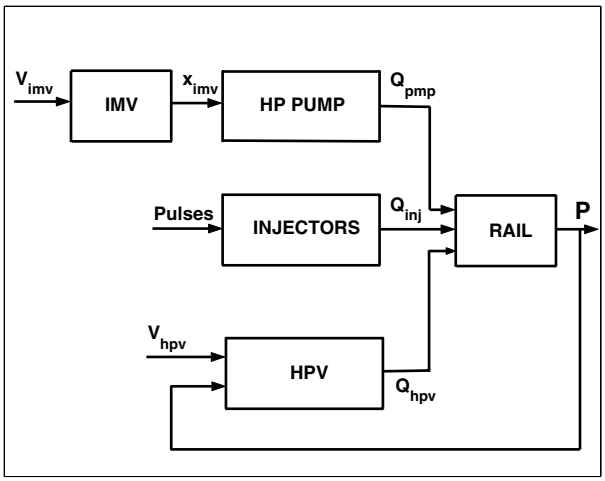

Figure 2

Synoptic of the system.

Note that the complete non linear model in Gauthier *et al.* (2005) is a 9th-order system.

The rail is a tank in which the fuel is pressurized. The hydraulic equations based model proposed in Gauthier *et al.* (2005) uses two physical characteristics of the rail: the volume V [m^3], and the bulk modulus K [Pa]. Let us recall that the bulk modulus is a fuel feature describing the behavior of the rail pressure variation against flows, *i.e.* the higher K is, the more the rail pressure is sensitive to the flow variation inside the rail. The physical rail model is as follows:

$$\frac{dP}{dt} = \frac{K(P,T)}{V}\left(Q_{pmp} - Q_{inj}\right)dt \tag{1}$$

This model is non linear since the bulk modulus K depends on the rail pressure and the fuel temperature, as shown in Figure 3.

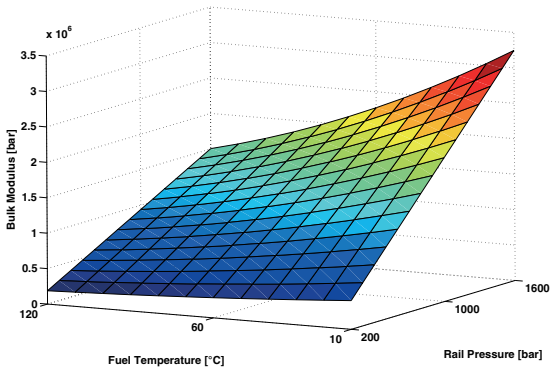

Figure 3

The bulk modulus variation against rail pressure and the fuel temperature.

To achieve a high performance and robustness level for the whole range of pressure and fuel temperature values, the bulk modulus variation should be taken into account in the control design. In this work, this is done using an LPV model of the Common Rail system considering the pressure, temperature and engine speed as varying parameters.

1.3 The Common-Rail LFT model

For control design purpose, this non linear model is first linearized and represented as a LFT model by pulling out the varying parameters (variable) into the Θ matrix as described later. First, let System (2) be the non linear Common Rail system, represented by system (2)

$$\begin{aligned} x_{k+1} &= f\left(x_k, u_k, p_1, p_2, ..., p_i\right) \\ y_k &= g\left(x_k, u_k, p_1, p_2, ..., p_i\right) \end{aligned} \tag{2}$$

where x is the state vector, u the control input and p_j ($j = 1, ..., i$) are the system parameters (*i.e.* engine speed, fuel temperature, etc.). The linearized model is

$$\begin{aligned} x^\star_{k+1} &= \frac{\partial f}{\partial x}x^\star_k + \frac{\partial f}{\partial u}u^\star_k \\ y^\star_k &= \frac{\partial g}{\partial x}x^\star_k + \frac{\partial g}{\partial u}u^\star_k \end{aligned} \tag{3}$$

$$\begin{aligned} x^\star_{k+1} &= A\left(p_1, p_2, ..., p_i\right)x^\star_k + B\left(p_1, p_2, ..., p_i\right)u^\star_k \\ y^\star_k &= C\left(p_1, p_2, ..., p_i\right)x^\star_k + D\left(p_1, p_2, ..., p_i\right)u^\star_k \end{aligned} \tag{4}$$

Then by scaling each parameter p_j such that $p_j = \delta_{j0} + \theta_j\delta_j$ with

$$\begin{aligned} \delta_{j0} &= \frac{max(p_j) + min(p_j)}{2} \\ \delta_j &= \frac{max(p_j) - min(p_j)}{2} \\ \left|\theta_j\right| &\leq 1 \end{aligned} \tag{5}$$

and pulling out θ_j forming $\Theta = diag(\theta_1, \theta_2, ..., \theta_i)$, one gets the LFT model which is valid for the whole operating domain.

The corresponding LFT representation is shown Figure 4 (where P may also include weighting functions used for control synthesis) with the state-space model

$$\begin{pmatrix} x_{k+1} \\ q_\theta \\ z_k \\ y_k \end{pmatrix} = \begin{pmatrix} A & B_\theta & B_1 & B_2 \\ C_\theta & D_{\theta\theta} & D_{\theta 1} & D_{\theta 2} \\ C_1 & D_{1\theta} & D_{11} & D_{12} \\ C_2 & D_{2\theta} & D_{21} & D_{22} \end{pmatrix} \cdot \begin{pmatrix} x_k \\ \omega_\theta \\ r_k \\ u_k \end{pmatrix} \tag{6}$$

where $x_k \in \Re^{n_a}$ are the states of the plant, $q_\theta \in \Re^{n_\theta}$ the variables entering the Θ block, $z_k \in \Re^{n_z}$ the controlled outputs, $y_k \in \Re^{n_y}$ the measures, $\omega_\theta \in \Re^{n_\theta}$ the inputs coming from

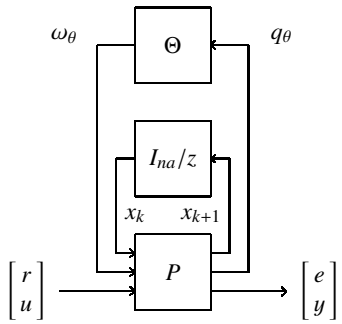

Figure 4

Plant LFT representation, Θ is the diagonal parameter matrix.

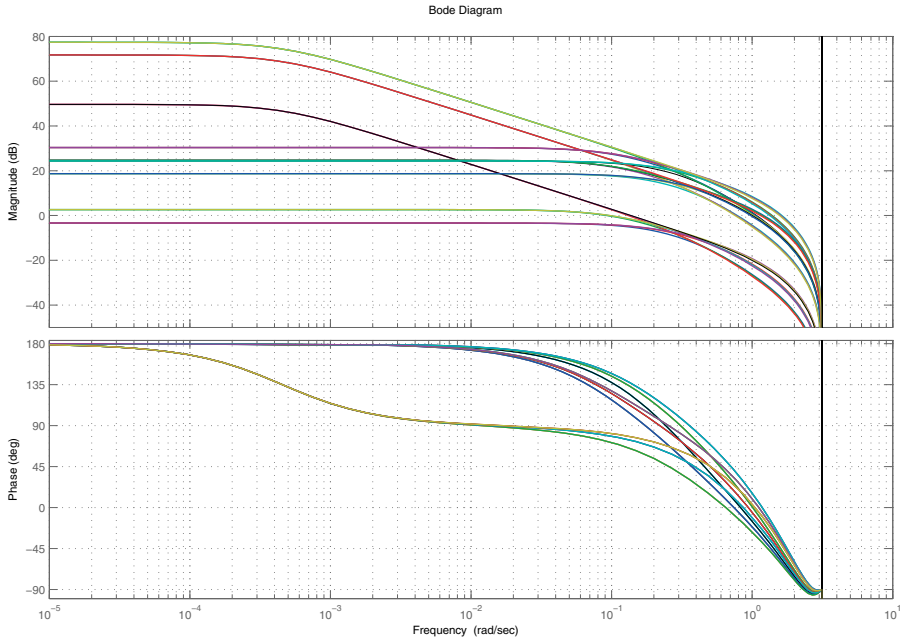

Figure 5

Plant behaviour according to Θ variation.

the Θ block, $r \in \Re^{n_r}$ the reference inputs of the system and $u \in \Re^{n_u}$ the control inputs. $P(z)$ is the upper LFT interconnection between P and I_{na}/z and the LPV plant $P_\Theta(z)$ is the upper LFT interconnection between $P(z)$ and Θ.

$$P(z) = F_u(P, I_{na}/z),\ P_\Theta(z) = F_u(P(z), \Theta) \tag{7}$$

Remark: if necessary, uncertainties could also be included in such a representation.

In Figure 5 the Bode diagram of the transfer function $y(z)/u(z)$ is plotted w.r.t. the parameter variations, *i.e.* $\Theta_j \in \{-1, 0, 1\}$, $j = 1, 2, 3$.

This shows that the considered system has large gain and bandwidth variations according to the parameter values.

2 DISCRETE-TIME H_∞ LFT CONTROLLER

In this section the method to design the $\mathcal{H}_\infty$/LPV controller, in an LFT form, is developed. The methodology is presented for discrete-time systems, which is a straightforward extension of the result in (Apkarian and Gahinet, 1995) for continous-time systems.

The goal of the LFT control is to take into account the set of varying-parameters Θ in the same way as $P_\Theta(z)$, hence

$$u = F_l(K(z), \Theta)\, y \tag{8}$$

The controller state-space representation *(Fig. 6)* is

$$\begin{pmatrix} x_{k+1}^c \\ u_k \\ q_\theta^c \end{pmatrix} = \begin{pmatrix} A_k & B_{k1} & B_{k\theta} \\ C_{k1} & D_{k11} & D_{k1\theta} \\ C_{k\theta} & D_{k\theta 1} & D_{k\theta\theta} \end{pmatrix} \cdot \begin{pmatrix} x_k^c \\ y_k \\ \omega_\theta^c \end{pmatrix} \tag{9}$$

with $x_k^c \in \Re^{n_k}$ the states of the controller, $u \in \Re^{n_u}$ the controller output, $q_\theta^c \in \Re^{n_\theta}$ the outputs going to Θ block, $y \in \Re^{n_y}$ the controller input, and $\omega_\theta^c \in \Re^{n_\theta}$ the input coming from Θ block.

$K(z)$ is the upper LFT interconnection between K and I_{nk}/z, and the LPV controller $K_\Theta(z)$ is defined by

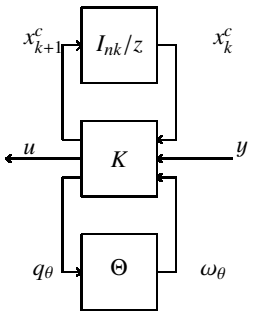

Figure 6

Controller LFT representation.

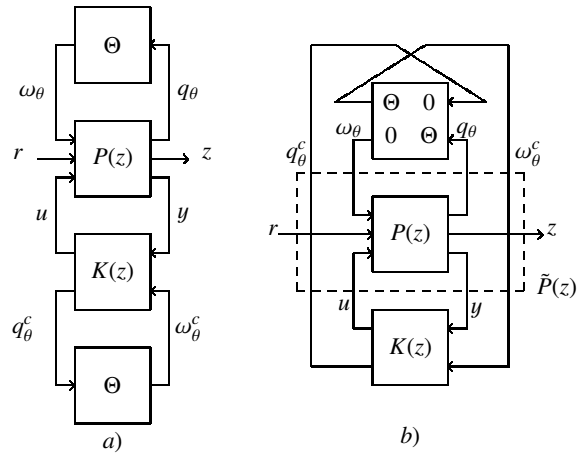

Figure 7

LFT control scheme.

the lower LFT interconnection between $K(z)$ and Θ

$$K(z) = F_u(K, I_{nk}/z),\ K_\Theta(z) = F_l(K(z), \Theta) \tag{10}$$

The closed-loop system from the external input r to the controlled output z is given by

$$T(P, K, \Theta) = F_l(P_\Theta(z), K_\Theta(z)) \tag{11}$$

Finally, the LFT control form is shown in Figure 7a. After a slight transformation, the system can be represented as shown in Figure 7b. The aim of the LFT control is to find a controller $K(z)$ such that the linear parameter varying system $T(P, K, \Theta)$ is stable.

The $\mathcal{H}_\infty$ control problem for a LPV plant is formulated as follows: find a controller K(z) such that the LPV controller $K_\Theta(z)$ satisfies:

– The closed-loop system (11) is internally stable for all parameter trajectories θ_i such that $|\theta_i| < 1$
– The induced $\mathcal{L}_2$-norm between r and z satisfies

$$\left\| \frac{z}{r} \right\|_\infty < \gamma \tag{12}$$

To reduce the conservatism due to the presence of uncertainties, the problem is usually reformulated using some scaling variables. Hence, the gain-scheduled $\mathcal{H}_\infty$ LFT control problem is defined as follows: *find a LTI controller $K(z)$ such that the following inequality is satisfied:*

$$\left\| \begin{bmatrix} L^{1/2} & 0 \\ 0 & 1/\sqrt{\gamma} \end{bmatrix} T(P(z), K(z)) \begin{bmatrix} L^{-1/2} & 0 \\ 0 & 1/\sqrt{\gamma} \end{bmatrix} \right\|_\infty < 1 \tag{13}$$

where L is a scaling matrix (see Apkarian and Gahinet, 1995) for more details about the L matrix characteristics). The solution of this problem is given by the following theorem, which is a straightforward extension of the result obtained in the continuous time domain case in (Apkarian and Gahinet, 1995) to the discrete-time domain case.

Theorem 1 *Consider a discrete-time LPV plant $P_\Theta(z)$ represented by the form (6-7). Let $\mathcal{N}_r$ and $\mathcal{N}_s$ denote bases of null spaces of $(B_2^T, D_{\theta 2}^T, D_{12}^T, 0)$ and $(C_2, D_{2\theta}, D_{21}, 0)$, respectively. Let $L = \begin{pmatrix} L_1 & L_2 \\ L_2^T & L_3 \end{pmatrix}$ and $J = L^{-1} = \begin{pmatrix} J_1 & J_2 \\ J_2^T & J_3 \end{pmatrix}$. With this notation, the gain-scheduled $\mathcal{H}_\infty$ LFT control problem is solvable if and only if there exist pairs of symmetric matrices $(R, S) \in \mathfrak{R}^{n_a \times n_a}$ and $(L_3, J_3) \in \mathfrak{R}^{n_\theta \times n_\theta}$ and a scalar $\gamma > 0$ such that*

$$\mathcal{N}_r^T \begin{pmatrix} ARA^T - R + B_\theta J_3 B_\theta^T & \star \\ C_\theta RA^T + D_{\theta\theta} J_3 B_\theta^T & C_\theta RC_\theta^T + D_{\theta\theta} J_3 D_{\theta\theta}^T - J_3 \\ C_1 RA^T + D_{1\theta} J_3 B_\theta^T & C_1 RC_\theta^T + D_{1\theta} J_3 D_{\theta\theta}^T \\ B_1^T & D_{\theta 1}^T \\ \star & \star \\ \star & \star \\ C_1 RC_1^T + D_{1\theta} J_3 D_{1\theta}^T - \gamma I & \star \\ D_{11}^T & -\gamma I \end{pmatrix} \mathcal{N}_r < 0$$

$$\mathcal{N}_s \begin{pmatrix} A^T SA - S + C_\theta^T L_3 C_\theta & \star \\ B_\theta^T SA + D_{\theta\theta}^T L_3 C_\theta & B_\theta^T SB_\theta + D_{\theta\theta}^T L_3 D_{\theta\theta} - L_3 \\ B_1^T SA + D_{\theta 1}^T L_3 C_\theta & B_1^T SB_\theta + D_{\theta 1}^T L_3 D_{\theta\theta} \\ C_1 & D_{1\theta} \\ \star & \star \\ \star & \star \\ B_1^T SB_1 + D_{\theta 1}^T L_3 D_{\theta 1} - \gamma I & \star \\ D_{11} & -\gamma I \end{pmatrix} \mathcal{N}_s < 0$$

$$\begin{pmatrix} R & I \\ I & S \end{pmatrix} > 0 \tag{14}$$

$$L_3\Theta = \Theta L_3,\ J_3\Theta = \Theta J_3,\ \begin{pmatrix} L_3 & I \\ I & J_3 \end{pmatrix} > 0 \tag{15}$$

Proof: The proof is a straightforward application of the result in the continuous time domain case in (Apkarian and Gahinet, 1995) applied in the discrete-time domain case. It is developed in more details in (Gauthier *et al.*, 2007).

3 ANTI-WINDUP COMPENSATOR DESIGN

Many works on the design of anti-windup compensation schemes (Edwards and Postlethwaite, 1999; Peng and Weller, 1998) have been done, in particular in the LMI framework (Mulder and Morari, 2001; Grimm *et al.*, 2003). The usual representation of such schemes is given in Figure 8, where the AW block can be a simple gain or a transfer function. In the present work, one uses an LFT representation of the anti-windup compensation similar to the one proposed in (Mulder and Morari, 2001), and a unique formulation of the designed discrete-time LPV/H_∞ control with anti-windup compensation is provided. Contrarily to (Mulder and Morari, 2001; Grimm *et al.*, 2003) where the

method is limited to stable open-loop systems, the compensation is chosen here to get smooth performance degradation of the controller gain, allowing to tackle open-loop unstable systems.

The objective of the anti-windup compensator is to minimize the $\mathcal{H}_\infty$ norm of the transfer function of the LPV controller with input(s) y and output(s) u.

Theorem 2 *Let $\tilde{K}$ be the augmented controller defined by the state space representation (16)*

$$\begin{pmatrix} x_{k+1}^c \\ u_k \\ q_\theta^c \end{pmatrix} = \begin{pmatrix} A_k & B_{1k} & B_{2k} & B_{3k} \\ C_{1k} & D_{11k} & D_{12k} & 0 \\ C_{2k} & D_{21k} & D_{22k} & D_{23k} \end{pmatrix} \begin{pmatrix} x_k^c \\ y_k \\ \omega_\theta^c \\ \Delta_s u_k \end{pmatrix} \tag{16}$$

with $\left[B_{3k}^T, D_{23k}^T\right]^T = \nabla$ the anti-windup gain, and N_{aw} be the null space of $(0.5C_1, 0.5D_{11}, 0.5D_{12}, I, 0)$. The gain ∇ minimizes the controller gain (in a sense defined later in (27)) if and only if there exist matrices $X_{aw} \in \Re^{n_k \times n_k}$, $L_{aw} \in \Re^{n_\theta \times n_\theta}$ and a scalar $\gamma_s > 0$ solution of the LMI

$$\mathcal{N}_{aw}^T \begin{pmatrix} A_k^T X_{aw} A_k - X + C_{2k}^T L_{aw} C_{2k} \\ B_{1k}^T X_{aw} A_k + D_{21k} L_{aw} C_{2k} \\ B_{2k}^T X_{aw} A_k + D_{22k} L_{aw} C_{2k} \\ 0 \\ 0 \\ 0 \end{pmatrix} \begin{pmatrix} \star \\ B_{1k}^T X_{aw} B_{1k} + D_{21k}^T L_{aw} D_{21k} - \gamma_s I \\ B_{2k}^T X_{aw} B_{1k} + D_{22k}^T L_{aw} D_{21k} \\ 0 \\ 0 \\ 0 \end{pmatrix}$$

$$\begin{pmatrix} \star & \star & \star & \star \\ \star & \star & \star & \star \\ B_{2k}^T X_{aw} B_{2k} + D_{22k}^T L_{aw} D_{22k} - L & \star & \star & \star \\ 0 & -\gamma_s I & \star & \star \\ 0 & 0 & -\gamma_s I & \star \\ 0 & 0 & 0 & -\gamma_s I \end{pmatrix} \mathcal{N}_{aw} < 0$$

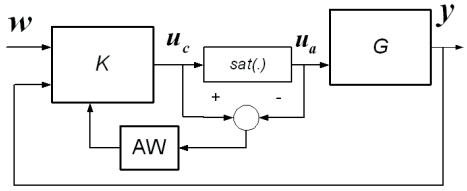

Figure 8

Anti-windup compensation scheme.

$$\begin{pmatrix} -X_{aw} & \star & \star & \star & \star & \star \\ 0 & -\gamma_s I & \star & \star & \star & \star \\ 0 & 0 & -L_{aw} & \star & \star & \star \\ 0 & 0 & 0 & -\gamma_s I & \star & \star \\ C_{1k} & D_{11k} & D_{12k} & 0 & -\gamma_s I & \star \\ 0.5C_{1k} & 0.5D_{11k} & 0.5D_{12k} & 0 & 0 & -\gamma_s I \end{pmatrix} < 0 \tag{17}$$

$$X_{aw} > 0,\ L_{aw}\Theta = \Theta L_{aw} \text{ and } L_{aw} > 0 \tag{18}$$

The proof is given in Appendix.

4 SIMULATION

The discrete-time $\mathcal{H}_\infty$ LFT anti-windup controller is validated on a fine non linear Diesel Engine Common Rail Injection model, see (Gauthier *et al.*, 2005) for more details. The model is driven by experimental input data obtained from a real vehicle.

4.1 $\mathcal{H}_\infty$ LFT Controller Result

Figure 9 shows the result of an $\mathcal{H}_\infty$ LFT synthesis. On the upper graph, the sensibility function $r \to e$ (r: reference, $e = r - y$) is plotted. On the lower graph, the controller transfer ($y \to e$) is plotted. All the plots depend on the Θ parameters.

Note that the sensitivity functions are quite similar for all parameter values (allowing to get similar performances for all parameter variations), while the controllers need to be different, to cope with the variation of the open loop system behaviour.

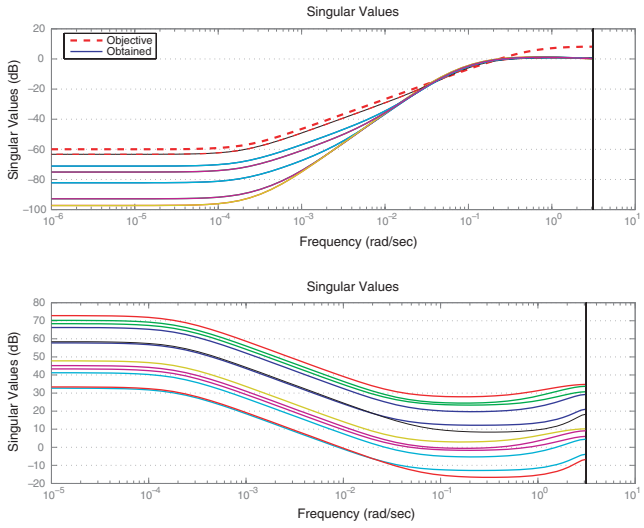

Figure 9

Upper plot: sensibility function $r \to e$ according to Θ parameter, lower plot: controller transfer according to Θ parameter.

4.2 Anti-Windup Effect

Figure 10 clearly shows the reduction of the controller gain for a given set of parameters Θ with Θ_s varying from -0.9 up to 1. The closer to 1 Θ_s is, the more the gain is reduced.

4.3 Simulation Results of the LFT Anti-Windup Control

To illustrate both the LFT control and the anti-windup compensator, two tests (among others) are made. The first one emphasizes the anti-windup effect (some parameters are fixed) while the second one shows both LFT controller and anti-windup acting (parameters, *e.g.* engine speed, injected fuel demand, etc., vary in a wide interval).

Figure 11 (upper and lower plots) clearly shows the benefit of the anti-windup compensation. The controller takes into account the command saturation and modifies its behavior to preserve stability. Figures 12 and 14 show both the rail pressure control and the actuator opening, with and without anti-windup compensator. Obviously, the two controls have the same behavior until the command reaches the maximum output value. At this time, with the anti-windup compensator, the controller output is kept close to the saturation value (see *Fig. 14*, solid line) and the closed loop system is stable (see upper plot in *Fig. 12*, solid line). In the other case, *i.e.* without the anti-windup compensator, the controller output reaches much higher values (see *Fig. 14*, dotted line) and the system becomes unstable (see upper plot in *Fig. 12*, dotted line). The control is then no longer efficient.

The according parameter variations are shown in Figure 13.

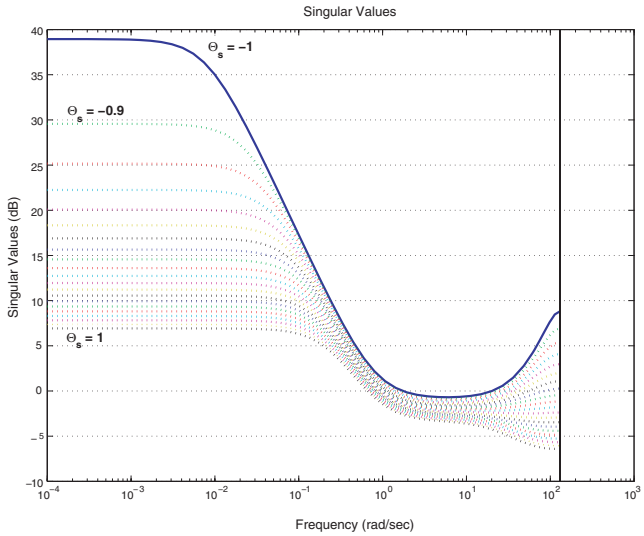

Figure 10

Anti-windup compensation effect on the controller gain; solid line: no compensation; dotted lines: compensation ($\Theta_s \in [-0.9, 1]$).

4.4 Comparison with Gain-Scheduling PID Controller

The actual control strategy embedded on car is a gain-scheduled PID, which is compared here to the designed $\mathcal{H}_\infty$ LFT controller.

The measured engine variables are the rail pressure reference, the engine speed, the fuel demand and the fuel temperature. We also pick up the rail pressure feedback from the vehicle to compare with the proposed rail pressure feedback result.

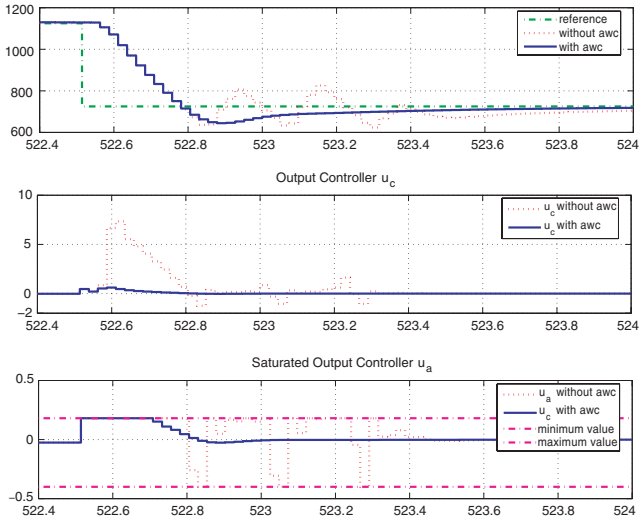

Figure 11

Test 1: Rail pressure control both with and without anti-windup compensation (awc).

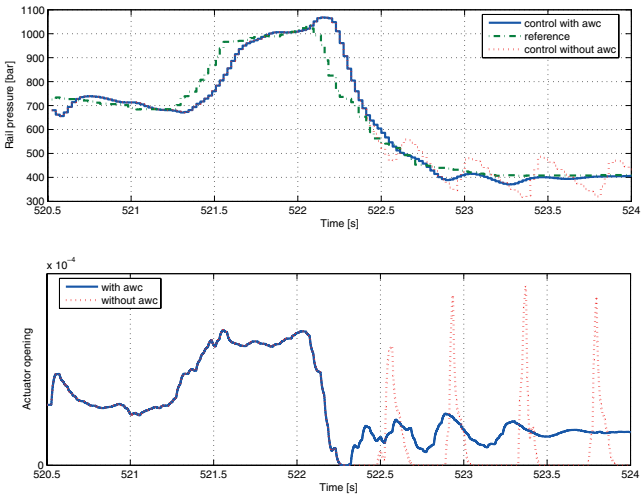

Figure 12

Test 2: Rail pressure control both with and without anti-windup compensation (awc).

Figure 15 shows both the rail pressure feedback from simulation and vehicle for a same reference and the corresponding variations of the engine speed and fuel demand are shown in Figure 16 (which is the origin of the disturbance Q_{inj}).

The $\mathcal{H}_\infty$ LFT controller responds faster than the gain-scheduled PID controller. Therefore, the rail pressure error is reduced during transients.

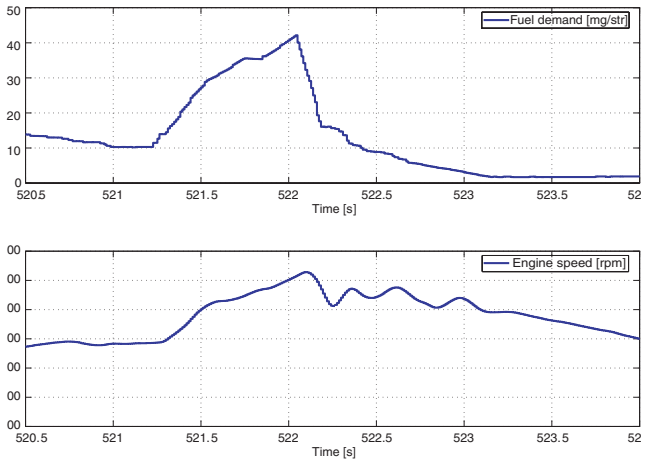

Figure 13

Test 2: Fuel demand [mg per stroke] and engine speed [round per minute].

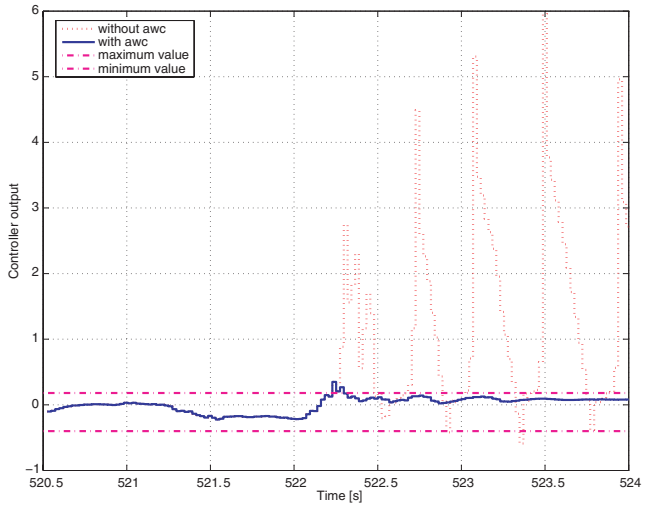

Figure 14

Test 2: Controller output both with and without anti-windup compensation (AWC).

CONCLUSIONS

In this paper, a discrete-time $\mathcal{H}_\infty$ LPV anti-windup controller has been developed in the LFT framework. The control design was divided into two parts: the $\mathcal{H}_\infty$ LFT control design and then the anti-windup compensator design. For the latter, a smooth degradation of the controller gain was achieved, allowing thus to tackle open-loop unstable systems. Finally, this method introduces a LFT controller that takes into account both real parameters (*e.g.* engine speed, injected fuel demand, etc.) and the saturation parameters. Some preliminary simulation results on a fine non linear model show all the interest of the developed methodology.

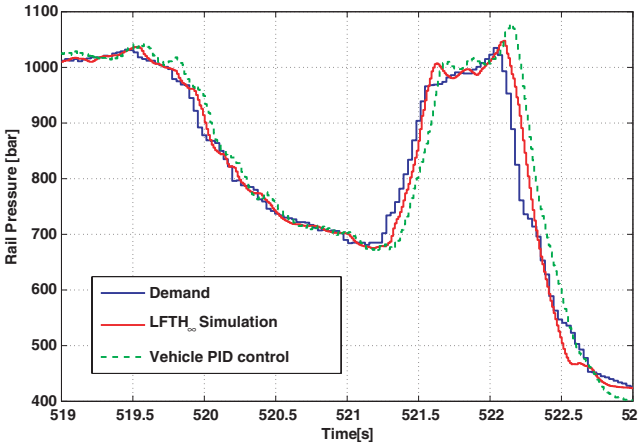

Figure 15

Rail pressure control result.

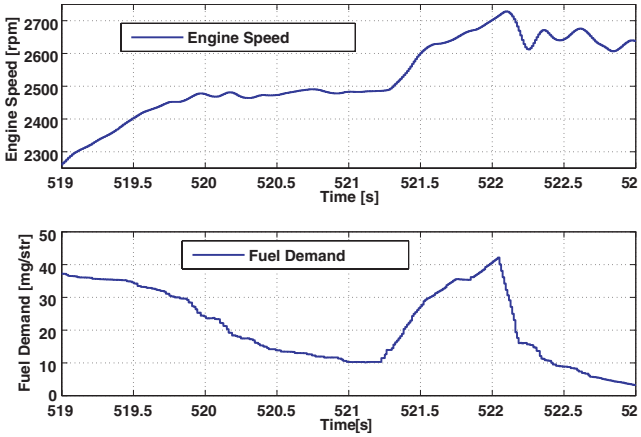

Figure 16

Engine speed and fuel demand.

Compared to classical approaches, the advantages are the following:

– When the vehicle characteristics are changed, the design of a LFT controller is quite easy compared to PID strategy which is more time consuming since it requires new identification steps and controller gains calibration and verification.

– The robust control theory used in the LFT approach ensures the performance and stability of the closed-loop system for all parameter values and variations. This is much more involved to check for gain-scheduled PID controllers.

– The provided simulation results emphasize the better performance of the developed methodology, compared to a gain-scheduled PID controller.

APPENDIX

Proof: The anti-windup compensator design problem is presented in Figure 17a.

To obtain a convex LMI formulation of the problem, one defines $\Delta_s = 0.5 + \Theta_s \cdot 0.5$, with $\Theta_s \in \Re$ and $|\Theta_s| < 1$, $q_\theta^{c'} = \Theta_s \omega_\theta^{c'}$ and pulls out Θ_s as an uncertainty parameter. This notation leads to the Figure 17b with $\tilde{K}'$ defined as follows:

$$\begin{pmatrix} x_{k+1}^c \\ u_k \\ \tilde{q}_\theta^c \end{pmatrix} = \begin{pmatrix} \bar{A}_k & \bar{B}_{1k} & \bar{B}_{2k} \\ C_{1k} & D_{11k} & \bar{D}_{12k} \\ \bar{C}_{2k} & \bar{D}_{21k} & \bar{D}_{22k} \end{pmatrix} \begin{pmatrix} x_k^c \\ y_k \\ \tilde{\omega}_\theta^c \end{pmatrix} \tag{19}$$

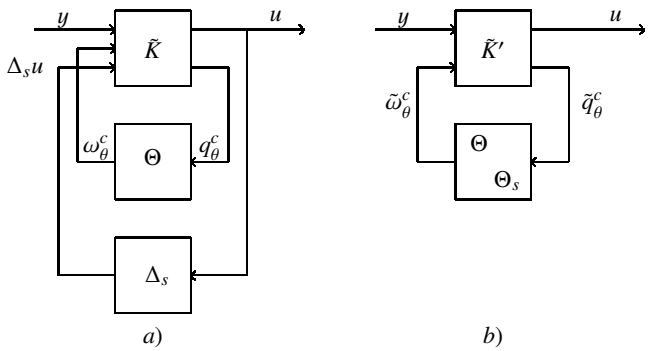

Figure 17

Anti-windup scheme.

with $\tilde{q}_k^c = \left(q_\theta^c, q_\theta^{c'}\right)^T$, $\tilde{\omega}_\theta^c = \left(\omega_\theta^c, \omega_\theta^{c'}\right)^T$ and:

$$\begin{aligned} \bar{A}_k &= A_k + 0.5 B_{3k} C_{1k} \\ \bar{B}_{1k} &= B_{1k} + 0.5 B_{3k} D_{11k} \\ \bar{B}_{2k} &= (B_{2k} + 0.5 B_{3k} D_{12k}, B_{3k}) \\ \bar{D}_{12k} &= \begin{pmatrix} D_{12k} & 0 \end{pmatrix} \\ \bar{C}_{2k} &= \begin{pmatrix} C_{2k} + 0.5 D_{23k} C_{1k} \\ 0.5 C_{1k} \end{pmatrix} \\ \bar{D}_{21k} &= \begin{pmatrix} D_{21k} + 0.5 D_{23k} D_{11k} \\ 0.5 D_{11k} \end{pmatrix} \\ \bar{D}_{22k} &= \begin{pmatrix} D_{22k} + 0.5 D_{23k} D_{12k} & D_{23k} \\ 0.5 D_{12k} & 0 \end{pmatrix} \end{aligned} \tag{20}$$

with $\nabla = \left(B_{3k}^T, D_{23k}^T\right)^T$, we define:

$$\begin{aligned} A_{kcl} &= \bar{A}_k \\ &= A_k + U \nabla \tilde{C}_{1k} \\ &= \tilde{A}_k + U \nabla \tilde{C}_{1k} \end{aligned} \tag{21}$$

with $U = \begin{pmatrix} I & 0 \end{pmatrix}$ et $\tilde{C}_{1k} = 0.5 C_{1k}$,

$$\begin{aligned} B_{kcl} &= \begin{pmatrix} \bar{B}_{1k} & \bar{B}_{2k} \end{pmatrix} \\ &= \tilde{B}_k + U \nabla \tilde{D}_{1k} \end{aligned} \tag{22}$$

with $\tilde{B}_k = \begin{pmatrix} B_{1k} & B_{2k} & 0 \end{pmatrix}$ and
$\tilde{D}_{1k} = \begin{pmatrix} 0.5 D_{11k} & 0.5 D_{12} & 1 \end{pmatrix}$

$$\begin{aligned} C_{kcl} &= \begin{pmatrix} C_{1k} \\ \tilde{C}_{2k} \end{pmatrix} \\ &= \tilde{C}_{2k} + V \nabla \tilde{C}_{1k} \end{aligned} \tag{23}$$

with $\tilde{C}_{2k} = \begin{pmatrix} C_{1k} \\ C_{2k} \\ 0.5 C_{1k} \end{pmatrix}$ et $V = \begin{pmatrix} 0 & 0 \\ 0 & I \\ 0 & 0 \end{pmatrix}$,

$$\begin{aligned} D_{kcl} &= \begin{pmatrix} D_{11k} & \bar{D}_{12} \\ \bar{D}_{21k} & \bar{D}_{22k} \end{pmatrix} \\ &= \tilde{D}_{2k} + V \nabla \tilde{D}_{1k} \end{aligned} \tag{24}$$

with $\tilde{D}_{2k} = \begin{pmatrix} D_{11k} & D_{12k} & 0 \\ D_{21k} & D_{22k} & 0 \\ 0.5 D_{11k} & 0.5 D_{12k} & 0 \end{pmatrix}$.

These notations lead to state space representations (25) and (26) for $\tilde{K}'$,

$$\begin{pmatrix} x_{k+1}^c \\ \tilde{u}_k \end{pmatrix} = \begin{pmatrix} \tilde{A}_k + U \nabla \tilde{C}_{1k} & \tilde{B}_k + U \nabla \tilde{D}_{1k} \\ \tilde{C}_{2k} + V \nabla \tilde{C}_{1k} & \tilde{D}_{2k} + V \nabla \tilde{D}_{1k} \end{pmatrix} \begin{pmatrix} x_k^c \\ \tilde{y}_k \end{pmatrix} \tag{25}$$

where $\tilde{u}_k$ is defined by the controller outputs u_k and $q_\theta^{c'}$, and $\tilde{y}_k$ by the controller inputs y_k and $\omega_\theta^{c'}$.
i.e.,

$$\begin{pmatrix} x_{k+1}^c \\ \tilde{u}_k \end{pmatrix} = \begin{pmatrix} A_{kcl} & B_{kcl} \\ C_{kcl} & D_{kcl} \end{pmatrix} \begin{pmatrix} x_k^c \\ \tilde{y}_k \end{pmatrix} \tag{26}$$

One defines $T_{kcl}(z) = \left(D_{kcl} + C_{kcl}\,(zI - A_{kcl})^{-1}\,B_{kcl}\right)$ and the following objective

$$\left\| \begin{pmatrix} L_{aw}^{1/2} & 0 \\ 0 & 1/\sqrt{\gamma_s} \end{pmatrix} T_{kcl} \begin{pmatrix} L_{aw}^{-1/2} & 0 \\ 0 & 1/\sqrt{\gamma_s} \end{pmatrix} \right\|_\infty < 1 \tag{27}$$

In the same way as the $\mathcal{H}_\infty$ LFT controller solution, the scaled bounded real lemma is applied to the system (27) with the notations of the system (25). Then one obtains the following LMI:

$$\Psi_{aw} + H_{aw}^T \nabla Q_{aw} + Q_{aw}^T \nabla^T H_{aw} < 0 \tag{28}$$

where

$$\Psi_{aw} = \begin{pmatrix} -X_{aw} & \tilde{A}_k & \tilde{B}_k & 0 \\ \tilde{A}_k^T & -X_{aw} & 0 & \tilde{C}_{2k}^T \\ \tilde{B}_k^T & 0 & -\mathcal{L}_{aw} & \tilde{D}_{2k}^T \\ 0 & \tilde{C}_{2k} & \tilde{D}_{2k} & -\mathcal{L}_{aw}^{-1} \end{pmatrix} \tag{29}$$

$$H_{aw} = \begin{bmatrix} U^T & 0 & 0 & V^T \end{bmatrix},\ Q_{aw} = \begin{bmatrix} 0 & \tilde{C}_{1k} & \tilde{D}_{1k} & 0 \end{bmatrix} \tag{30}$$

The inequality (28) has a solution ∇ if and only if

$$W_{awh}^T \Psi_{aw} W_{awh} < 0 \qquad W_{awq}^T \Psi_{aw} W_{awq} < 0 \tag{31}$$

The development of the two LMIs (31) leads to the LMIs of *Theorem 2*. Once X_{aw}, L_{aw} and γ_s are solved, Ψ_{aw} is computed and the anti-windup compensator ∇ is obtained by solving the LMI (28).

REFERENCES

Apkarian, P. and Gahinet, P. (1995) A convex characterizatoin of gain-scheduled $\mathcal{H}_\infty$ controllers. *IEEE Trans. Automat. Contr.*, **40**, 853-864.

Edwards, C. and Postlethwaite, I. (1999) An anti-windup scheme with closed-loop stability considerations. *Automatica*, **35**, 761-765.

Mulder, E.F., Kothare, M.V. and Morari, M. (2001) Multivariable anti-windup controller synthesis using linear matrix inequalities. *Automatica*, **37**, 1407-1416.

Gauthier, C., Sename, O., Dugard, L. and Meissonnier, G. (2005) Modelling of a diesel engine common rail injection system. *IFAC 16th World Congress*, Prague.

Gauthier, C., Sename, O., Dugard, L. and Meissonnier, G. (2007) An $\mathcal{H}_\infty$ linear parameter-varying (LPV) controller for a diesel engine common rail injection system. *European Control Conference ECC*, Kos, Greece.

Gissinger, G. and Le Fort-Piat, N. (2002) *Contrôle-commande de la voiture*, Lavoisier.

Grimm, G., Hatfield, J., Postlethwaite, I., Teel, A.R., Turner, M.C. and Zaccarian, L. (2003) Antiwindup for stable linear systems with input saturation: an LMI-based synthesis. *IEEE T. Automat. Contr.*, **48**, 1509-1525.

Guerrassi, N., Schoeppe, D., Bercher, Ph. and Spadafora, P. (2002) Common rail injection system design and strategies for low emissions diesel vehicles. *2nd Int. Conf. on Advanced Automotive Diesel Engine Technology*, *SAE-China*, pp. 125-133.

Guerrassi, N. and Dupraz, P. (1998) A common rail injection system for high speed direct injection diesel engines. *SAE No. 980803*.

Jung, M. and Glover, K. (2006) Calibrated linear parameter-varying control of a turbocharged diesel engine'. *IEEE Trans. Contr. Syst. Tech.*, **1**, 45-62.

Kiencke, U. and Nielsen, L. (2000) *Automotive Control Systems*, Springer.

van Nieuwstadt, M. (2002) Modeling and control of diesel powertrains, in *Vehicle Modelling and Control*, European summer school in automatic control of Grenoble, France.

Peng, Y., Vrancic, D., Hanus, R. and Weller, S.S.R. (1998) Anti-windup designs for multivariable controllers. *Automatica*, **34**, 1559-1565.

Zhang, F., Grigoriadis, K.M., Franchek, M.A. and Makki, I.H. (2005) Linear parameter-varying lean burn air-fuel ratio control. *Proc. 44th IEEE Conf. on Decision and Control, and the European Conference and Control, 2005*, Seville, Spain.

Final manuscript received in October 2006